1 Introduction

Oceanic gravity waves fundamentally contribute to the redistribution of mechanical energy in the world ocean. The wave energy pathways can be altered in a result of interaction with large scale sea bottom features such as submarine mountains, trenches and continental slopes. These processes shape wave propagation, cause energy dissipation and thus give rise to variation in the energy budgets. In this work, by means of numerical simulations, energy scattering of tsunamis and internal waves of tidal frequency (internal tides) is examined for realistic cases of their interaction with ocean's bottom relief.

Tsunami is a transient wave impulsively forced by submarine earthquakes. The waves traverse vast expanses of the oceans and encounter numerous sea bottom features (Mofjeld et al., 2001). Such interaction with Hawaiian-Emperor seamount chain and Hess Rise diverts energy from initially uniform propagation (Kowalik et al., 2008; Tang et al., 2012). Now wave intensity is focused into tight, "pencil" beams that later lead to diverse waveforms in far-field. This is observed as numerous wave trains arriving in irregular sequence and with drastic changes in magnitude. For example, during the 2011 Tohoku-oki tsunami observations made by tidal gauges on the US West Coast clearly demonstrated spatial-temporal variation of tsunami surges (Borrero & Greer, 2013) such that some of the largest waves unexpectedly appeared with a several hour delay after the leading wave. This problem is investigated in the Chapter 1. Scattering by Koko Guyot, the largest submarine seamount in the Emperor chain (Figure 1), is studied in order to quantify and provide description for the observed far-field signals during two recent tsunami events: the 2006 Kuril and 2011 Tohoku-oki tsunamis.

The second problem considered here explores internal waves that pervade ocean's interior. Their existence owns to water column stratification since these waves manifest as an oscillatory motion of isopycnal surfaces. The initial perturbation can be forced by different mechanisms: wind stress (Garrett, 2001), buoyancy flux (Garrett & Munk, 1979), ice ridge keels (Morison, 1986) or even tsunami (Santek & Winguth, 2007). As well, tidal currents at steep topography brings existence of internal tides. These are baroclinic waves that oscillate with tidal or quasi-tidal frequency.

One reason to study baroclinic tides is their role in dissipation of barotropic, surface tidal energy (Munk, 1997). Current estimates suggest that 1/3 of total tidal energy is converted into internal motions in the deep ocean (Egbert & Ray, 2000). From this roughly 1/3 is directly lost to turbulent mixing right at generation sites (St. Laurent & Garrett, 2002) while the rest is emitted as freely propagating waves in form of tight beams (Simmons et al., 2004; Zhao et al., 2016). These structures are observed to cross the ocean basins without much attenuation. This finding fuels scientific research to understand where and how the baroclinic tidal energy is dissipated. Since the deposition sites primarily would occur deep below direct wind influence, the internal tides are thought to be a candidate for providing mechanical energy to close the upwelling branch of Meridional overturning circulation (Munk & Wunsch, 1998). Regardless of global importance, the baroclinic tides are relevant for local processes such as water mass transformation (Stigebrandt & Aure, 1989), vertical nutrient fluxes (Sharples et al., 2007), sediment (Hotchkiss & Wunsch, 1982) and larvae transports (Pineda, 1999).

All of the above is crucially dependent on internal-tide generation, propagation and scatter-

ing that are still poorly constrained. The Tasman Tidal Dissipation Experiment (TTIDE) had its goal to provide description of the internal tide reflection in relatively simple setting of Tasman continental slope. An internal tidal beam originated at Macquarie Ridge, New Zealand transverses Tasman Sea and impinges on the slope of Tasmania (Figure 1). The primary aim is to quantify amount of wave energy being reflected back into open sea, scattered into higher vertical modes and consequently, describe processes associated with sink of energy. These problems are addressed in Chapters 2 and 3.
The two geophysical problems examined in the thesis represent a wave scattering by inhomogeneity in propagation media. Here, it takes form of rapid change in ocean depth imposing constrains on fluid motion. The accompanying transfers are intrinsically linked to energy flux approach. This is reviewed in **Section 2** by considering a normal mode dynamics, while **Section 3** describes energy characteristics associated with wave transformations caused by interaction with bathymetry.

2 Normal modes in flat-bottom sea

Tsunami and internal tides are a case of long gravity waves. Their typical wavelengths are order of 100 km being larger than the ocean's mean depth. So the wave dynamics can be well described in linear, hydrostatic framework. As first step, the wave propagation is discussed for flat-bottom ocean. The equations of motion in stratified, Boussinesq ocean on an f-plane (Kundu & Cohen, 2008; Cushman-Roisin & Beckers, 2011) will take mathematical form of,

$$\frac{\partial u}{\partial t} - fv = -\frac{1}{\bar{\rho}_0}\frac{\partial p}{\partial x} \tag{1}$$

$$\frac{\partial v}{\partial t} + fu = -\frac{1}{\bar{\rho}_0}\frac{\partial p}{\partial y} \tag{2}$$

$$0 = -\frac{\partial p}{\partial z} - \rho g \tag{3}$$

$$N^2 w = -\frac{1}{\bar{\rho}_0}\frac{\partial^2 p}{\partial z \partial t} \tag{4}$$

$$\frac{\partial u}{\partial x} + \frac{\partial v}{\partial y} + \frac{\partial w}{\partial z} = 0 \tag{5}$$

with $(u,\ v,\ w)$ being velocity along zonal, meridional and vertical axis, f - Coriolis parameter, p - perturbation pressure arising either from sea level oscillations or isopycnal displacements within stratified water column given by Brunt-Vaisala frequency $N^2 = -\frac{g}{\bar{\rho}_0}\frac{\partial \rho_0}{\partial z}$. Additionally, boundary conditions are imposed on the surface and bottom,

$$w|_{z=0} = \frac{\partial \zeta}{\partial t},\ p|_{z=0} = \bar{\rho}_0 g \zeta \tag{6}$$

$$w|_{z=-H} = 0 \tag{7}$$

The both conditions are of linear form since the sea level motions are much smaller than the acceleration due to gravity, and the ocean depth is fixed. Such formulated problem allows separation of vertical motions by employing following decomposition,

$$(u,v,p)(x,y,z,t) = \sum_{n=0}[u_n(x,y,t), v_n(x,y,t), p_n(x,y,t)]\psi_n(z) \tag{8}$$

$$w(x,y,z,t) = \sum_{n=0}[w_n(x,y,t)]\int_{-H}^{z}\psi_n(z)dz \tag{9}$$

$$\rho(x,y,z,t) = \sum_{n=0}[\rho_n(x,y,t)]\frac{d\psi_n(z)}{dz} \tag{10}$$

Upon substitution Sturm-Liouville problem is obtained for vertical structure (basis) functions $\psi_n(z)$[1],

$$\frac{d}{dz}\left(\frac{1}{N^2}\frac{d\psi_n}{dz}\right) + \frac{1}{c_n^2}\psi_n = 0 \tag{11}$$

[1] note this is for horizontal variables, usually it is written for vertical velocity since boundary conditions are expressed right away

with an eigenvalue for a respective n-th vertical mode given by c_n. This is a phase speed in non-rotating ocean with an equivalent depth, D_n such that $\sqrt{gD_n} = c_n$. The carried out decomposition detaches vertical motions from horizontal dynamics reducing the initial set (1) to Laplace tidal equations,

$$\frac{\partial \vec{u}_n}{\partial t} + f\vec{k} \times \vec{u}_n = -\frac{1}{\rho_0}\nabla p_n \tag{12a}$$

$$\frac{1}{\rho_0}\frac{\partial p_n}{\partial t} + gD_n \nabla \cdot \vec{u}_n = 0 \tag{12b}$$

This states dynamical equivalence between barotropic, surface wave and baroclinic, internal waves if the ocean stratification would be absent and the apparent depth would be D_n. In actuality, 0-th mode represents a barotropic solution with vertically uniform dynamics ($\psi_0 = const$) and the equivalent depth $D_0 \simeq H$ (Hendershott, 1981). This mode resembles pure surface wave propagation such as in tsunami wave problem. The infinite sequence of higher vertical modes are internal modes that produce negligible sea level perturbations. This allows complete separation between barotropic and baroclinic motions which is similar to imposing rigid lid condition on internal modes (Kundu & Cohen, 2008).
The main interest is in linear wave phenomena, so harmonic temporal behavior $e^{i\omega t}$ will be implied leading to Helmholtz equation,

$$(\omega^2 - f^2)p_n + c_n^2 \Delta p_n = 0 \tag{13}$$

Making a plane wave ansatz, $e^{-i\vec{k}\cdot\vec{x}}$, currents and pressure will be related as

$$\begin{aligned} p_n &= p_{0n} e^{i(\omega t - \vec{k}\cdot\vec{x})} \\ u_n &= \frac{1}{\bar{\rho}_0}\frac{\omega k_x + i f k_y}{\omega^2 - f^2} p_n \\ v_n &= \frac{1}{\bar{\rho}_0}\frac{\omega k_y - i f k_x}{\omega^2 - f^2} p_n \end{aligned} \tag{14}$$

Than from (12b), a dispersion relation for Sverdrup waves follows,

$$\omega^2 = f^2 + c_n^2 |\vec{k}|^2 \tag{15}$$

The waves are dispersive as a result of Earth's rotation with phase and group speeds are

$$c_p = (1 - \frac{f^2}{\omega^2})^{-1/2} c_n,\ c_g = (1 - \frac{f^2}{\omega^2})^{1/2} c_n,\ c_p c_g = c_n^2 \tag{16}$$

For the most energetic mode-1 semidiurnal internal tide, phase travels with speed of 4 m/s, but group speed is only 2 m/s. So slow traveling wave is inevitably affected by background oceanic circulation. On contrary, tsunami waves exhibit shallow-water, nondispersive behavior with phase and group speeds of $\sim O(100\ m/s)$ owing to small periods in comparison to inertial period. Tsunami waves cross ocean basins in a matter of hours without any appreciable interaction with ocean's dynamical state.

In deep ocean, where bottom's topography does not demonstrate large spatial gradients, normal modes are an useful approach in description of wave-intensity changes. In order to do so energy equation can be developed from (12). Multiplying momentum equations by $\vec{u}_n$ and continuity equation by p_n, adding both expressions and depth integrating one obtains

$$(E_k + E_p)_t + \nabla \cdot \vec{F} = 0 \tag{17}$$

Additionally, depth averaging is carried out so that energy flux will be defined,

$$\vec{F}_n = \frac{1}{H} \vec{u}_n(t) p_n(t) \int_{-H}^{0} \psi^2(z) dz \tag{18}$$

For tsunami wave propagation due to their barotropic nature $\psi(z) = const$ and $p_n = \rho_0 g \eta$, the expression takes its classical form for surface wave propagation (Henry & Foreman, 2001), $\vec{F} = \rho_0 g \vec{u} \zeta$.
In internal tide studies period averaging further simplifies calculations,

$$\vec{F}_n = \frac{1}{2} \vec{u}_n^{\star} p_n \int_{-H}^{0} \psi^2(z) dz \tag{19}$$

where velocity and baroclinic pressure are now complex amplitudes of harmonic fit and * is a complex conjugate.
The obtained expressions for energy flux comprises only pressure-work term, i.e. transport of energy is dictated by pressure forces. In full formulation this is augmented with nonlinear contributions made by advection and dissipative forces (Gill, 2016). These terms are negligible presuming deep ocean propagation where the wave's spatial dimensions are large and magnitude of dynamical variables is small.
Away from scattering region, an energy budget could be constructed following the linearized normal mode dynamics. Any loss in intensity of primary wave has to be balanced by energy scattered into other wave motions and by dissipative losses. The latter is not discussed here and thought to be comprised by residue terms. While the scattered wave field, reflected components and intermodal conversion are the main topic of investigation. The quantitative aspects are discussed in **Section 3**.

3 Oceanic wave scattering

The normal mode approach was formulated under the assumption of flat bottom with a simplified boundary condition, $w|_{z=-H} = 0$ that allows separation of variables. Thence, vertical motions are decoupled from horizontal dynamics. As a wave encounters an inclined slope the simplified relation does not hold and the bottom boundary condition becomes nonlinear,

$$(\vec{u} \cdot \nabla h)|_{z=-h(x,y)} = 0 \text{ or } w = -\vec{u}_h \cdot \nabla h \tag{20}$$

The condition states that there is no mass transport across an impermeable bottom. The wave motion cannot alone satisfy (20), and a compensating flow has to develop to preserve mass. For the configuration when an incident wave train encounters a vertical wall in nonrotating ocean, a specular reflection occurs in order to fulfill the no-flow condition. Opposing fluid motions will be produced by a back-scattered wave.

An additional condition is imposed on scattered waves such that the energy vanishes with distance (Mei et al., 1989; Morse & Feshbach, 1946). The Sommerfeld radiation condition leads to a far-field asymptotic:

$$p_{scat} \sim \frac{e^{i\vec{k}\cdot\vec{x}}}{|\vec{x}|}\Phi_s(\theta) \tag{21}$$

This is an assertion for circularly spreading waves having some angular distribution Φ_s, called a scattering amplitude. The squared quantity will furnish amount of scattered radiation. In the problem of tsunami-topography interaction, far-field signals could be approximated with the above distributions; while in internal tide reflection problem, large distances away (when continental slope becomes a point) an angularly integrated scattered amplitude will be directly related to a reflection coefficient, though wave spreading with distance has to be factored in.

In the near-field, a scattered wave field can be decomposed by Fourier transform whereby each wavenumber can be regarded as a separate component. As it propagates away, it will begin to separate from others. Magnitude modulations due to interference [2] will subdue. And at large distances, respective Fourier coefficient will represent a scattering amplitude in direction corresponding to the wave vector. As a result, Fourier transform depicts the far-field's distribution of energy.[3]

In addition to angular scattering, there could occur a transfer of energy into different vertical modes. Let us consider a long wave that obeys Laplace tidal equations entering a region where bottom slope is inclined and the full boundary condition (20) has to be satisfied. It only can be fulfilled if there is a vertical velocity. A normal mode by itself is not able to represent the dynamics since the vertical derivative, by definition, is zero on the boundary. However, a superposition of modes can force horizontal convergence to cancel out the vertical velocity. Physically, pressure gradients should develop by displacing isopycnal surfaces which further radiate energy away in the form of baroclinic modes. In general, this describes a coupled-mode approach (Griffiths & Grimshaw, 2007). Locally-flat normal modes counteract one another through the boundary condition. The spatial gradients will dictate mode's magnitude to equilibrate the balance. Dynamically, Laplace tidal equation for each separate mode will embrace an additional force represented as intermodal-coupling term (Griffiths & Grimshaw, 2007; Kelly et al., 2016).

The intermodal conversion and energy flux carried by modes can be estimated as work done by vertical velocity against modal pressure, $W_{m\to n} \sim (w_{m,\ scat}\ p_n)|_{z=-h} = -((\vec{u}_m \cdot \nabla h)p_n)|_{z=-h}$. But total conversion must as well account for the opposite energy transfer, from n to m, hence,

$$C_{m\to n} = -((\vec{u}_m \cdot \nabla h)\ p_n)|_{z=-h} + ((\vec{u}_n \cdot \nabla h)\ p_m)|_{z=-h} \tag{22}$$

[2] more appropriate to say diffraction

[3] This is a fundamental idea in acoustic holography (Williams, 1999), should I cite other fields?.

Internal tide excitation can be viewed as scattering of barotropic tide by steep relief (Hendershott, 1981). If the surface tide is the 0^{th} mode, then energy lost can be diagnosed as

$$C_{bt\to bc} = -(\vec{u}_{bt} \cdot \nabla h) \sum_{n=1} p_n|_{z=-h} \tag{23}$$

assuming that the baroclinic wave field effect on surface tide is negligible (Kelly et al., 2012). The above expression is well established in internal tide studies (Kurapov et al., 2003; Llewellyn Smith & Young, 2002; Pickering et al., 2015).
For consideration of mode-1 scattering it is useful to reformulate (22) by employing Leibniz's rule, the continuity equation per each normal mode, and mode's orthogonality,

$$C_{m\to n} = \int_{-h}^{0} (u_m \nabla p_n - u_n \nabla p_m) dz \tag{24}$$

In the problem of internal wave propagation over uniform and gently inclined bottom (Wunsch, 1968), there is no intermodal conversion, $C_{m\to n} = 0$, and each mode's dynamics is perfectly matched by presence of others. Strictly speaking, in this case the wave equation is hyperbolic [4] and propagation occurs along characteristics (Sandstrom, 1969) or internal wave rays described by

$$\gamma = \frac{dz}{dx} = \pm \frac{\omega^2 - f^2}{N^2 - \omega^2} \tag{25}$$

Slope criticality can be defined as ratio between its inclination and rays angle, γ. In subcritical regime of forward propagation, the ratio is less than unity. In this case for steeper bottom more higher modes is necessary to describe internal tide dynamics (Figure 2). Now it is apparent that a mode conversion will not happen, unless there is a change in topography to drive adjustment of mode amplitudes. On contrary, in supercritical regime, when $\nabla h > \gamma$, internal waves are reflected with always present generation of higher modes. Usually, they will be phase-locked into vertically propagating rays (Garrett & Kunze, 2007; Lamb, 2014) subject to breaking and dissipation (Lien & Gregg, 2001; Nash et al., 2004; Klymak et al., 2011). In case of the continental slope this causes internal tide mode-1 reflection to decrease relative to the equivalent case of surface wave reflection.
As a first approximation for long waves scattering, it will be instructive to consider a problem with simplified geometry. This will usually consist of a step discontinuity connecting the deep ocean with the top of seamount (e.g. Koko Guyot) or the continental shelf. Then the boundary condition (20) is analogous to fulfilling so-called matching conditions (Mei et al., 1989). These are mass conservation and continuity of sea level for surface waves

$$\vec{u}_1 h_1 = \vec{u}_2 h_2,\ \zeta_1 = \zeta_2 \tag{26}$$

In the case of internal tides - continuity of pressure and no-flow through vertical walls (St. Laurent & Garrett, 2002; Larsen, 1969; Chapman & Hendershott, 1981), the conditions are

$$p_1 = p_2, -h_2 \le z \le 0 \tag{27}$$

$$\vec{u}_1 = 0, -h_1 \le z \le -h_2 \tag{28}$$

$$\vec{u}_1 = \vec{u}_2, -h_2 \le z \le 0 \tag{29}$$

[4](in contrary to elliptical Helmholtz equation, (13))

4 Organization of thesis

The thesis consists of the following three chapters:

Chapter 1 makes its goal analysis of scattering of tsunami waves by Koko Guyot. The approach is based on obtaining scattering amplitude (21), evaluation of its frequency and spatial characteristics in order to describe far-field signals. The discussion and conclusions are supported with analytical calculations based on matching conditions approach.

Chapter 2 deals with generation of semidiurnal internal tide at Macquarie Ridge, Tasman Sea. This is studied in a detail by analysis of three dimensional structure of internal wave field. The proposed mechanism explains peculiarities of conversion rates (23). The emitted internal tidal beam than described in the far-field with emphasis on its kinematic properties.

Chapter 3 concerns the tidal beam reflection from Tasman Continental Slope. The obtained energy levels show variability that is due to number of factors. Possibility of each is discussed and respective estimates are made in order to propose physically reasonable mechanism of internal tide dynamics in three dimensionally complex region.

Throughout the thesis a method based on inverse modeling was used. Its mathematical rudiments are given in Appendix A.

Figures

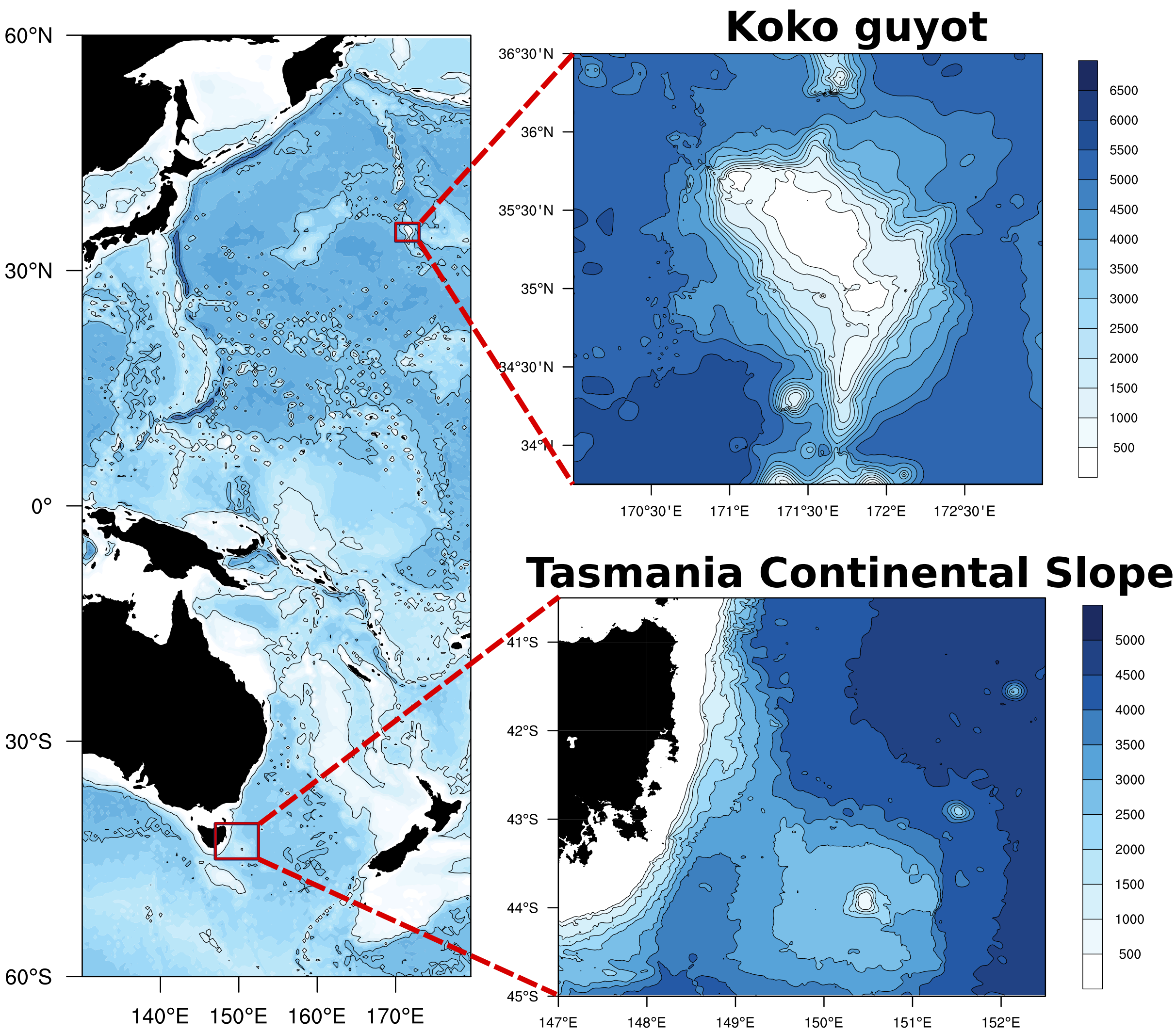

Figure 1: Bathymetric map of the Pacific Ocean with outlined regions showing geographic locations of considered wave scattering problems.

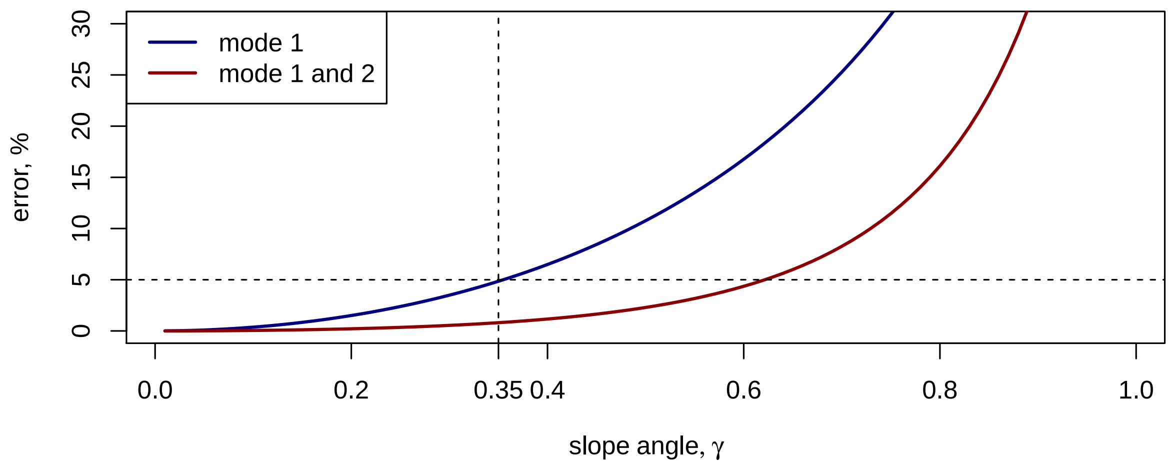

Figure 2: Error in description of internal wave structure by flat-bottom vertical modes as bottom gets steeper.

References

Borrero, J. C., & Greer, S. D. (2013, Jun 01). Comparison of the 2010 chile and 2011 japan tsunamis in the far field. *Pure and Applied Geophysics*, *170*(6), 1249–1274. Retrieved from `https://doi.org/10.1007/s00024-012-0559-4` doi: 10.1007/s00024-012-0559-4

Chapman, D. C., & Hendershott, M. C. (1981). Scattering of internal waves obliquely incident upon a step change in bottom relief. *Deep Sea Research Part A. Oceanographic Research Papers*, *28*(11), 1323–1338.

Cushman-Roisin, B., & Beckers, J.-M. (2011). *Introduction to geophysical fluid dynamics: physical and numerical aspects* (Vol. 101). Access Online via Elsevier.

Egbert, G., & Ray, R. (2000). Significant dissipation of tidal energy in the deep ocean inferred from satellite altimeter data. *Nature*, *405*(6788), 775–778.

Garrett, C. (2001). What is the near-inertial band and why is it different from the rest of the internal wave spectrum? *Journal of Physical Oceanography*, *31*(4), 962–971.

Garrett, C., & Kunze, E. (2007). Internal tide generation in the deep ocean. *Annu. Rev. Fluid Mech.*, *39*, 57–87.

Garrett, C., & Munk, W. (1979). Internal waves in the ocean. *Annual Review of Fluid Mechanics*, *11*(1), 339–369.

Gill, A. E. (2016). *Atmosphereocean dynamics.* Elsevier.

Griffiths, S. D., & Grimshaw, R. H. (2007). Internal tide generation at the continental shelf modeled using a modal decomposition: Two-dimensional results. *Journal of physical oceanography*, *37*(3), 428–451.

Hendershott, M. C. (1981). Long waves and ocean tides. *Evolution of physical oceanography*.

Henry, R., & Foreman, M. (2001). A representation of tidal currents based on energy flux. *Marine Geodesy*, *24*(3), 139–152.

Hotchkiss, F. S., & Wunsch, C. (1982). Internal waves in hudson canyon with possible geological implications. *Deep Sea Research Part A. Oceanographic Research Papers*, *29*(4), 415–442.

Kelly, S. M., Lermusiaux, P. F., Duda, T. F., & Haley Jr, P. J. (2016). A coupled-mode shallow-water model for tidal analysis: internal tide reflection and refraction by the gulf stream. *Journal of Physical Oceanography*, *46*(12), 3661–3679.

Kelly, S. M., Nash, J. D., Martini, K. I., Alford, M. H., & Kunze, E. (2012). The cascade of tidal energy from low to high modes on a continental slope. *Journal of Physical Oceanography*, *42*(7), 1217–1232.

Klymak, J. M., Alford, M. H., Pinkel, R., Lien, R.-C., Yang, Y. J., & Tang, T.-Y. (2011). The breaking and scattering of the internal tide on a continental slope. *Journal of Physical Oceanography*, *41*(5), 926–945.

Kowalik, Z., Horrillo, J., Knight, W., & Logan, T. (2008). Kuril islands tsunami of november 2006: 1. impact at crescent city by distant scattering. *Journal of Geophysical Research: Oceans (1978–2012)*, *113*(C1). doi: 10.1029/2007jc004402

Kundu, P., & Cohen, I. (2008). *Fluid mechanics. 2004.* Elsevier Academic Press.

Kurapov, A. L., Egbert, G. D., Allen, J., Miller, R. N., Erofeeva, S. Y., & Kosro, P. (2003). The m 2 internal tide off oregon: Inferences from data assimilation. *Journal of Physical Oceanography*, *33*(8), 1733–1757.

Lamb, K. G. (2014). Internal wave breaking and dissipation mechanisms on the continental slope/shelf. *Annual Review of Fluid Mechanics*, *46*, 231–254.

Larsen, L. H. (1969). Internal waves incident upon a knife edge barrier. In *Deep sea research and oceanographic abstracts* (Vol. 16, pp. 411–419).

Lien, R.-C., & Gregg, M. (2001). Observations of turbulence in a tidal beam and across a coastal ridge. *Journal of Geophysical Research: Oceans*, *106*(C3), 4575–4591.

Llewellyn Smith, S. G., & Young, W. (2002). Conversion of the barotropic tide. *Journal of Physical Oceanography*, *32*(5), 1554–1566.

Mei, C. C., Stiassnie, M., & Yue, D. K.-P. (1989). *Theory and applications of ocean surface waves: Part 1: Linear aspects part 2: Nonlinear aspects*. World Scientific.

Mofjeld, H., Titov, V., González, F., & Newman, J. (2001). Tsunami scattering provinces in the pacific ocean. *Geophysical research letters*, *28*(2), 335–337.

Morison, J. (1986). Internal waves in the arctic ocean: A review. In *The geophysics of sea ice* (pp. 1163–1183). Springer.

Morse, P. M., & Feshbach, H. (1946). *Methods of theoretical physics*. Technology Press.

Munk, W. (1997). Once again: once againtidal friction. *Progress in Oceanography*, *40*(1), 7–35.

Munk, W., & Wunsch, C. (1998). Abyssal recipes ii: energetics of tidal and wind mixing. *Deep Sea Research Part I: Oceanographic Research Papers*, *45*(12), 1977–2010.

Nash, J. D., Kunze, E., Toole, J. M., & Schmitt, R. W. (2004). Internal tide reflection and turbulent mixing on the continental slope. *Journal of Physical Oceanography*, *34*(5), 1117–1134.

Pickering, A., Alford, M., Nash, J., Rainville, L., Buijsman, M., Ko, D. S., & Lim, B. (2015). Structure and variability of internal tides in luzon strait*. *Journal of Physical Oceanography*, *45*(6), 1574–1594.

Pineda, J. (1999). Circulation and larval distribution in internal tidal bore warm fronts. *Limnology and Oceanography*, *44*(6), 1400–1414.

Rabinovich, A. B., Thomson, R. E., & Stephenson, F. E. (2006). The sumatra tsunami of 26 december 2004 as observed in the north pacific and north atlantic oceans. *Surveys in geophysics*, *27*(6), 647–677.

Sandstrom, H. (1969). Effect of topography on propagation of waves in stratified fluids. In *Deep sea research and oceanographic abstracts* (Vol. 16, pp. 405IN1407IN3409–406IN2408IN5410).

Santek, D., & Winguth, A. (2007). A satellite view of internal waves induced by the indian ocean tsunami. *International Journal of Remote Sensing*, *28*(13-14), 2927–2936.

Sharples, J., Tweddle, J. F., Mattias Green, J., Palmer, M. R., Kim, Y.-N., Hickman, A. E., ... others (2007). Spring-neap modulation of internal tide mixing and vertical nitrate fluxes at a shelf edge in summer. *Limnology and Oceanography*, *52*(5), 1735–1747.

Simmons, H. L., Jayne, S. R., Laurent, L. C. S., & Weaver, A. J. (2004). Tidally driven mixing in a numerical model of the ocean general circulation. *Ocean Modelling*, *6*(3), 245–263.

Stigebrandt, A., & Aure, J. (1989). Vertical mixing in basin waters of fjords. *Journal of Physical Oceanography*, *19*(7), 917–926.

St. Laurent, L., & Garrett, C. (2002). The role of internal tides in mixing the deep ocean. *Journal of Physical Oceanography*, *32*(10), 2882–2899.

Tang, L., Titov, V. V., Bernard, E. N., Wei, Y., Chamberlin, C. D., Newman, J. C., ... others (2012). Direct energy estimation of the 2011 japan tsunami using deep-ocean pressure measurements. *Journal of Geophysical Research: Oceans (1978–2012)*, *117*(C8).

Williams, E. G. (1999). *Fourier acoustics: sound radiation and nearfield acoustical holography*. Academic press.

Wunsch, C. (1968). On the propagation of internal waves up a slope. In *Deep sea research and oceanographic abstracts* (Vol. 15, pp. 251–258).

Zhao, Z., Alford, M. H., Girton, J. B., Rainville, L., & Simmons, H. L. (2016). Global observations of open-ocean mode-1 m2 internal tides. *Journal of Physical Oceanography*, *46*(6), 1657–1684.